EXPERIMENTAL INVESTIGATION OF THE EFFECTS OF CATHODE CURRENT ON HK40 HALL THRUSTER OPERATION

SPACE PROPULSION 2016
ROME, ITALY / 2–6 MAY 2016

Nazli Turan, Ugur Kokal, Murat Celik

Dept. of Mechanical Engineering, Bogazici University, Istanbul, Turkey
nazli.turan@boun.edu.tr, ugur.kokal@boun.edu.tr,
murat.celik@boun.edu.tr

KEYWORDS: electric propulsion, Hall effect thruster, cathode coupling

ABSTRACT:

Hall effect thrusters utilize electric and magnetic fields to extract ions from a plasma discharge. The cathode is responsible for the ionization of the propellant and the neutralization of the ion beam by emitting an equal number of electrons to prevent spacecraft charging. Hollow cathode electrons are extracted from LaB_6 insert surface by thermionic emission. The electrons leaving the surface generate a negative cathode voltage around LaB_6 emitter. As the emitter surface expels electrons, the same amount of electrons are attracted from the ground. Those electrons are measured as the ground current. For Hall effect thrusters, the electron movements are determined by the external magnetic lines of the thruster. If electrons could not pass the magnetic field lines, they could not reach the anode and the magnitude of cathode to ground voltage increases. As a result, plume plasma potential increases. This study shows that by measuring the electron current coming from the emitter surface, influence of the external magnetic field strength on the efficiency of the thruster could be predicted.

1. INTRODUCTION

Thrusters using electric energy have been built as a practical alternative to chemical thrusters due to their higher specific impulse and resulting lower propellant consumption for a given mission. After the huge impulse requirement of the spacecraft to be launched was handled, practical solutions have been investigated to utilize the onboard propellant more efficiently. Electric propulsion systems became a preferable option for certain planned long-term space missions, and researchers focused on satellites and spacecraft with electric propulsion broadly [1].

Hall effect thrusters (HET) use electric and magnetic fields to accelerate ions from plasma discharge. In Hall effect thrusters, a cathode emits electrons to ionize neutral atoms in the discharge channel and the created ions accelerate through the channel exit while electrons are partially trapped in the channel due to applied external magnetic field. The second role of the cathode is to emit equal amount of electrons to that of ejected ions to prevent the spacecraft from charging. Thus, cathode is a significant component of the HETs.

The proper operation of the thruster depends on the cathode characteristics such as emitter surface temperature, geometric parameters, keeper potential etc. Cathode emits electrons that form the discharge current; therefore it is part of the electric circuit of the thruster. Cathode voltage *(V_{cg})* is the potential difference between the inner region of the cathode tube and the common ground, and generated by the thermionic emission within the cathode tube. The potentials of anode and cathode generate discharge voltage *(V_d)*. Plasma potential *(V_p)* is measured in thruster plume. *(V_{pg})* is the difference between plasma potential and ground. Cathode coupling voltage *(V_c)* is defined as the potential difference between the plasma voltage and cathode voltage as in Fig.1. All the electrical components in the thruster are adjusted with respect to a common voltage. This common voltage is spacecraft itself in space or vacuum chamber walls on the ground [2].

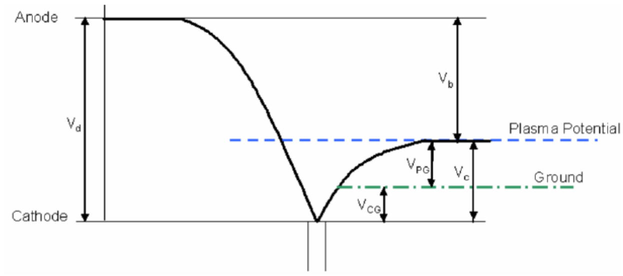

Figure 1. Hall effect thruster voltage schematic [3]

There is a relation between the cathode coupling voltage and thrust. The voltage that accelerates the ions *(V_b)* is calculated as the difference of the applied discharge voltage and cathode coupling voltage:

$$V_b = V_d - V_c \tag{1}$$

Also, the beam voltage *(V_b)* could be calculated as the difference between anode voltage and plasma potential, as the created ions are accelerated between anode voltage and plasma voltage. The plasma potential depends on the electrons supplied from the cathode, magnetic field, the placement of the cathode and the discharge characteristics.

In this study, plasma potential is measured with a Langmuir probe. Anode potential is observed by determining the discharge current. The cathode current is examined on the basis of current extracted from the ground to the LaB_6 emitter. Also, the current extracted from the common ground is investigated for different mass flow rates, heater currents and keeper currents when the thruster is off. Then, HK40 Hall effect thruster is operated at different operating conditions. To understand the mechanisms behind the plasma potential and the cathode potential, resistance analogy is used to explain the effects of magnetic field strength, cathode position, and the cathode characteristics such as keeper current, keeper voltage, insert temperature, geometry etc.

The relations between the magnetic field and the discharge properties are studied by considering the emitted electron current. The electron current from the cathode is observed to be lower than the discharge current. This means that the discharge current is predominantly formed by the electrons coming from the ionization of neutral Argon. Neutralization is assumed to be poor as there is insufficient number of electrons accompanying beam ions. Based on these observations, thrust and efficiency values are calculated analytically.

2. EXPERIMENTAL SETUP

2.1 Vacuum Facility

The tests have been conducted inside the Bogazici University Space Technologies Laboratory (BUSTLab) vacuum chamber. This vacuum chamber is a 1.5 m diameter 2.7 m long cylindrical tank. By using a mechanical pump and two cryogenic pumps, the pressure inside the vacuum chamber is maintained on the order of 3.2 x 10^{-5} Torr for 10 sccm Argon flow rate. In order to conduct experiments, various gas and electrical feedthroughs have been used to provide gas flow and power to inside the chamber.

2.2 HK40 Hall Thruster

HK40, designed and built at BUSTLab, is an SPT type Hall thruster with a dielectric channel outer diameter of 40 mm. In the latest design, the permanent magnets were replaced with magnetic coils. The coil currents are adjusted to different values for each experiment. At most, 1.7 A – 2.0 A are supplied to inner and outer coils, respectively. Magnetic field strength is measured with a Hall probe and the results are compared with COMSOL modeling of the thruster magnetic field topology and the model is optimized according to the measurements.

According to the magnetic topology model for the maximum current values, the maximum magnetic field strength in the channel is 380 G. The discharge voltage is measured to be 220 V with 1.2 A discharge current. A picture of the thruster inside the chamber before the tests is shown in Fig.2.

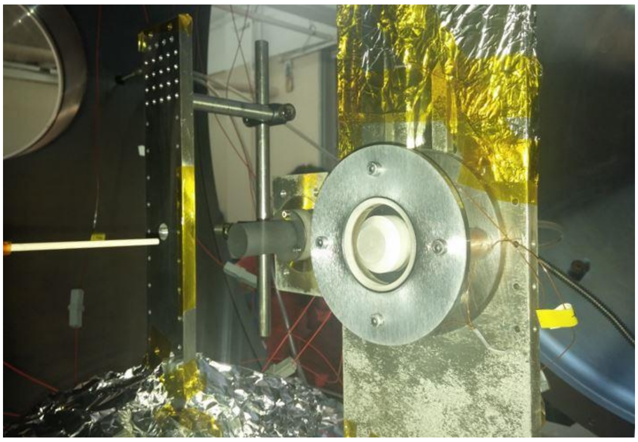

Figure 2. HK40 Hall thruster with moveable cathode

2.3 BUSTLab Hollow Cathode

The prototype hollow cathode, designed and built at BUSTLab, has a 6 mm diameter 48 mm long graphite cathode tube. It utilizes a 2 mm ID, 4 mm OD LaB_6 tube of 10 mm length as the thermionic emission material. The insert region of the cathode is heated using a heater that utilizes 0.25 mm (or 0.40 mm) diameter tantalum wire that is wrapped around a high temperature machinable ceramic (shapal) part that had external helical grooves.

2.4 Langmuir Probe

Plasma characteristics such as electron number density and electron temperature are measured by using a planar Langmuir probe with a 0.5 mm diameter tungsten wire inside an alumina tube. Plasma potential and floating potential are determined from the I-V curve. A Keithley 2410 sourcemeter is used for biasing the probe electrode and collecting current.

3. EXPERIMENTAL RESULTS

Experiments are conducted with different power sources for keeper, heater, anode, and inner and outer magnetic coils. During the tests, the cathode is placed axially, next to the thruster as seen in Fig.2. Argon gas at 2.2 sccm flow rate is supplied to the cathode for the first trials without operating HK40. Then, when the cathode operation becomes stable, the flow rate is reduced to 1.5 sccm for the nominal cathode operation. Argon propellant flow rate to the anode (thruster) is set to 18 sccm. At first, BUSTLab hollow cathode characteristics such as the relationship between the emitted electron current and the keeper current are studied. The effect of the heater on emitted current is observed by changing heater current. Then, the cathode is operated in self-heating mode. While the thruster is on, extracted current from the cathode and the anode voltage are observed for different magnetic coil currents. The Langmuir probe measurements are conducted on cathode plume and thruster plume when the thruster is in operation.

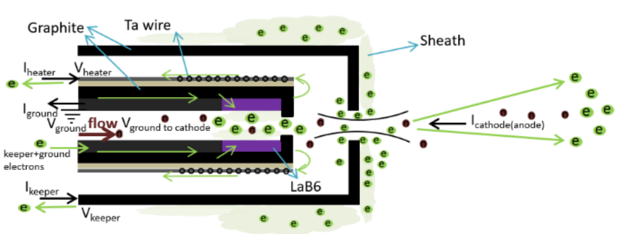

Figure 3. Schematic of the paths of currents and electrons

The source of the electrons that leave the cathode, thus providing the cathode current, is the LaB_6 insert located inside the cathode tube. As seen in Fig.3, the insert is at ground potential. As LaB_6 insert emits electrons, it would start attracting electrons from ground.

If the beam ion current could not be measured directly by a probe, there is a way to obtain beam current by considering that all electrons coming from the LaB_6 insert, which is at ground potential, move towards the anode through the discharge channel, and the ion beam has no divergence. A schematic of the currents in the thruster-cathode system is illustrated in Fig.4. Cathode emits electrons to ionize the propellant (I_{ec}) and to neutralize the expelled ion beam (I_{eb}) [2].

$$I_{cathode} = I_{ec} + I_{eb} \quad (2)$$

Cathode provides the primary electrons for the discharge current, and secondary electrons come from ionization (I_{ei}). These two currents constitute the discharge current as in Eq.3 [2]. The discharge current equals the total electron current:

$$I_d = I_{ec} + I_{ei} \quad (3)$$

Beam current (I_{ib}) is formed by ionization and the number of ions are equal to the electrons coming from ionization. Therefore,

$$I_d = I_{ib} + I_{ec} \quad (4)$$

Beam ions attract electrons to the thruster plume. Those electrons neutralize the beam. For the perfect neutralization case, the number of beam ions and the number of electrons provided to beam from the cathode are equal:

$$I_{ib} = I_{eb} \quad (5)$$

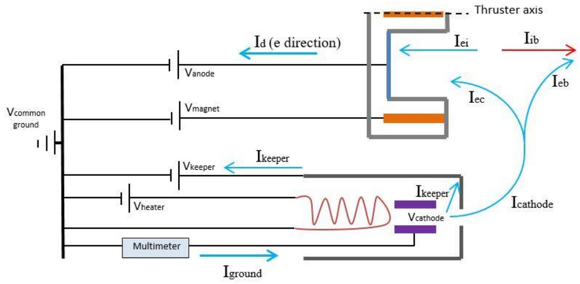

Figure 4. Schematic of the currents in the thruster-cathode system

As could be seen from Fig.4, in experiments when the electrons extracted from the ground are measured, this would include the supplied keeper current because all the parts in the cathode are at ground potential:

$$I_{ground} = I_{keeper} + I_{cathode} \qquad (6)$$

3.1 Cathode with continuous heating

BUSTLab hollow cathode is heated with a current of 6 A to provide sufficient current density for thermionic emission. This heater current is supplied gradually to protect the cathode materials from a possible cracking due to fast thermal expansion. After the cathode current emission is initiated, electrons emitted from the emitter surface ionize the Argon propellant inside the cathode tube. An electron-ion pair is obtained for each ionized Argon atom, which form a quasi-neutral plasma inside the cathode tube. The quasi-neutral plasma acts as a catalyst medium for the self-heating thermionic emission process. Electrons are much more energetic, thus they form a sheath on the LaB_6 inner surface and attract positively charged ions from the plasma. Electrons are pulled by the ions to the cathode plasma while ions are accelerated towards the inner wall, which provides a mechanism for continuous thermionic emission [4].

Inside the cathode tube, the self-heating mechanism causes the creation of a voltage difference between the plasma and the emitter surface. Due to the emitted electrons, the LaB_6 emitter's surface momentarily becomes positively charged creating a voltage difference between the inner surface of the LaB_6 insert and ground, which generates ground current *(I_{ground})*, which is measured. Cathode voltage is in an equilibrium in response to the continuous electron emission, which depends on the operating conditions, such as emitter material temperature and cathode propellant mass flow rate.

After the cathode is heated enough to provide sufficient current density of thermionic electron emission from the LaB_6 emitter's surface, keeper is biased to a high potential (~ 600 V) to attract electrons from the inner plasma. As the cathode discharge is initiated, the magnitude of keeper voltage drops depending on the propellant flow rate and the set keeper current value. In order to keep the cathode plasma as quasi-neutral, more electrons are extracted from the ground and the ground current to the LaB_6 increases. After the continuous electron emission in the plasma is properly initiated, keeper voltage arranges itself to the operational potential of the keeper at 20-50 V. Keeper current *(I_{keeper})* is also set to a desired value. At this step, heater current could be terminated. To protect the cathode materials from excessive heating and to minimize cathode energy consumption, the heater current should be turned off; however, it is left as turned-on to observe the effects of the heating process on the cathode currents.

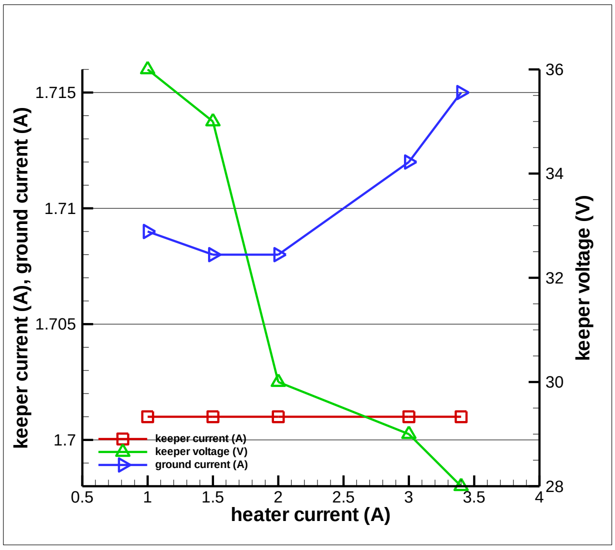

Figure 5. Cathode current for varying heater current

Higher temperature inside the cathode increases thermionic emission from the emitter surface, which increases the magnitude of cathode voltage. As would be explained later when discussing Fig.9, if the cathode voltage decreases, the keeper voltage arranges itself to a lower value to attract the same keeper current, as seen in Fig.5. Higher thermionic emission rate caused by high temperature causes a shift in the equilibrium resulting in a larger negative potential on the insert surface.

3.2 Cathode without heating

After the heater is turned off, the variation of the keeper current and keeper voltage are observed. For increased keeper current, extracted electrons *($I_{cathode}$)* increase as in Fig.6. On the contrary, an increase in the cathode flow rate causes a decrease in ground current. Fig.5 and Fig.7 could be compared to see the changes on ground current for a constant keeper current.

During the tests, a thin layer of glow is observed around the keeper. Electrons inside this layer of glow *($V_{keeper\ sheath}$)* shields the keeper voltage, therefore keeper voltage increases, in order to maintain keeper current at that level.

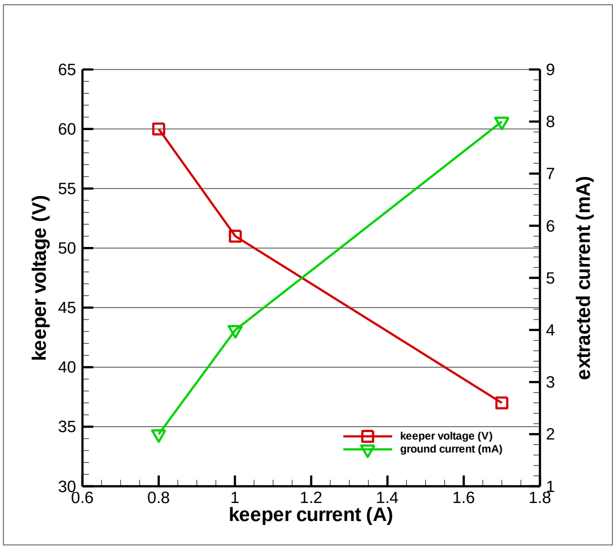

Figure 6. Changes in keeper voltage and extracted emission current from LaB_6 with respect to keeper current

If keeper current is increased, electrons in sheath layer contribute to the keeper current, and sheath layer disappears. As the sheath layer becomes thinner, keeper shielding decreases resulting in a decrease in keeper voltage as in Fig.6.

As the voltage difference between keeper and cathode voltages increases for higher keeper current values, more current is extracted from the ground. The cathode voltage becomes more negative if the plasma resistance between the keeper and LaB_6 surface is assumed to be constant (R_k in Fig.9).

3.3 Cathode with HK40 Hall thruster

After the thruster is operated, electrons are accelerated towards the anode. The magnetic coils of HK40 create magnetic field that causes the magnetization of the electrons. Electrons perform cyclotron motion around the magnetic field lines while moving axially to the anode. Electron-neutral collisions create Argon ions, and they are accelerated, by the decrease in potential, towards the outside of the discharge channel. In the acceleration region, electron temperature and plasma potential gradients along magnetic field lines are low. Therefore, the lines are considered as equipotential. The difference between the anode voltage and thruster plume plasma potential determines the beam voltage which determines the exhaust velocity. The processes are illustrated in Fig.8.

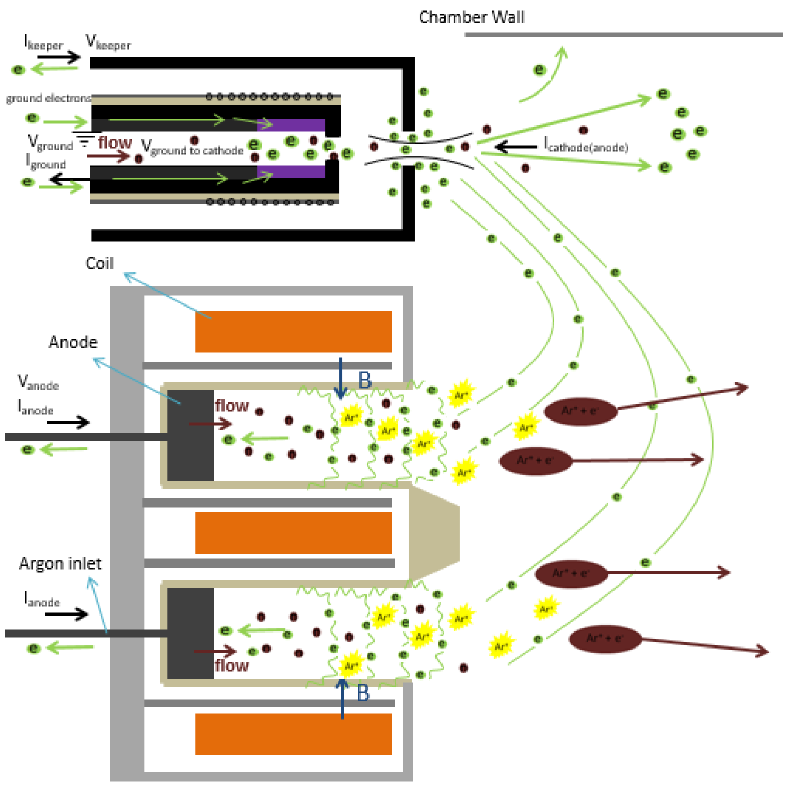

Figure 8. Schematic of the paths of electrons with ionization

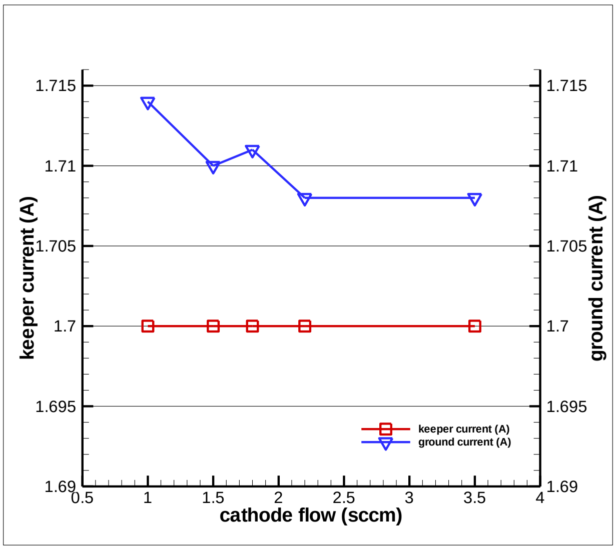

Figure 7. Cathode current for varying cathode propellant flow rate

Plume plasma potential is defined as the voltage at the thruster exit where the ion acceleration is completed. In order to illustrate the electrical circuit of the thruster-cathode system, a representative schematic is created as shown in Fig.9. The anode and the cathode can be characterized as a closed circuit where R_b, R_c, and R_k are the resistances between plasma and anode, plasma and cathode, and keeper and LaB_6 insert, respectively. R_b is created by the magnetic field topology in the discharge channel. R_c depends on the placement of the cathode as well as the external magnetic field of the thruster. R_k is the resistance between the cathode insert and the keeper.

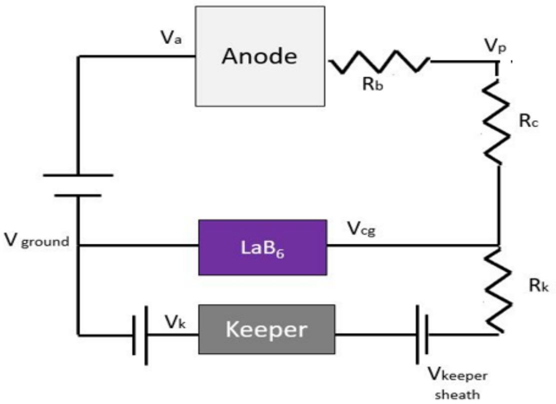

Figure 9. Representation of the electrical circuit for the thruster-cathode system

With an increase in magnetic field strength, anode voltage becomes higher. Ionization increases inside the channel due to increased number of collisions. Thus, the number of electrons coming from the ionization of the propellant increase. With constant discharge (anode) current, ground current (current from ground to the cathode) decreases (as seen in Fig.10), meaning that the electron current extracted from the cathode decreases. Plume plasma potential becomes higher for higher anode voltage because of the decrease in the number of electrons in the plume as seen in Fig.11. However, beam voltage, which is the difference between anode and plasma potentials increases because the increase in plasma potential is less than the increase in the anode voltage as in Fig.11. R_b increases by the strong magnetic field. Power transferred to the ion beam can be seen from the circuit diagram shown in Fig.9. The beam power is:

$$P_b = I_b(V_a - V_p) \tag{7}$$

Therefore, thrust increases for increased beam power, P_b, [5]. Thrust is given by:

$$T = \frac{I_b m_i}{e}\sqrt{2eV_b / m_i} \tag{8}$$

where m_i is the mass of the ion. Then, the efficiency could be calculated as:

$$\eta_T = \frac{1}{2}\frac{T^2}{\dot{m}_t P_t} \tag{9}$$

where $\dot{m}_t$ is the sum of mass flow rates to the anode and the cathode, and P_t is the total power which includes the power to anode, keeper and magnetic coils. The ratio of the beam kinetic power to the total power gives the efficiency as could be seen in Eq.9.

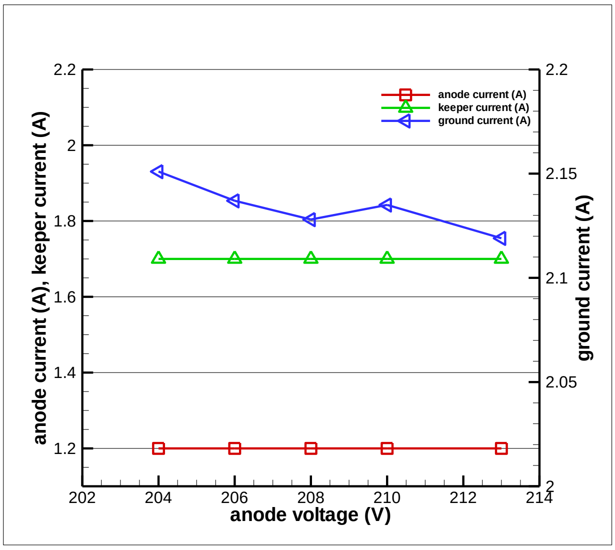

Figure 10. Current values for varying anode voltages

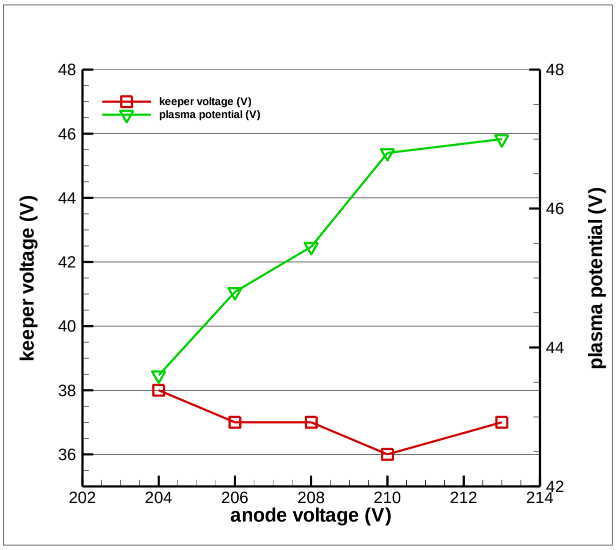

Figure 11. Keeper, plasma and floating voltage values for varying anode voltage values (probe data is taken at the thruster plume)

For some of the experiments, the currents to the inner and outer magnetic coils are varied. Data for five different inner and outer magnetic coil currents are presented in Fig.12. As seen in this figure, the electron current from the cathode *(I_{ec})* decreases with increased magnetic field. It could be asserted that electrons coming from ionization of Argon atoms *(I_{ei})* contribute to the discharge current more than the electrons extracted from the cathode. In this case, ion beam current *(I_{ib})* is higher than the electron current in the plume *(I_{eb})* and full neutralization is not achieved.

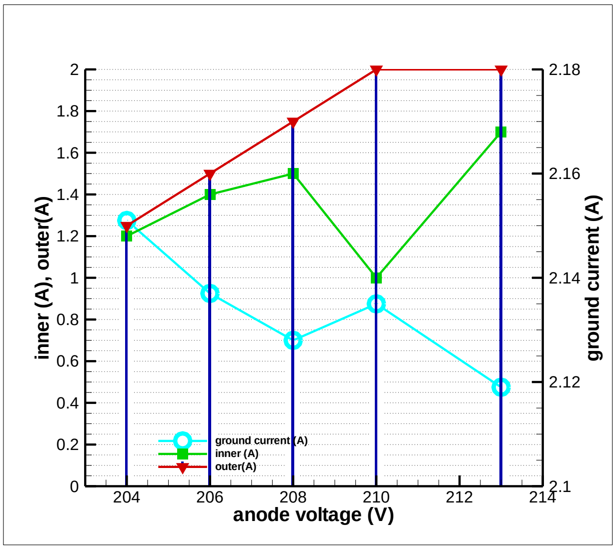

Figure 12. Extracted electron current from ground for various inner and outer magnet coil current values for varying anode voltages

4. MAGNETIC FIELD STRUCTURE

Using Eq's 2, 3 and 4, beam current is calculated from the measured discharge and cathode currents. The neutralizing electron current is assessed to be small because the discharge and the cathode currents are equal only for very low current values (around 0.3 A). The reason for this could be the non-uniform magnetic field topology created by the magnetic coils. Electron current is not sufficient to neutralize the expelled ions and a divergent plume is observed as shown in Fig.13 with magnetic contour lines taken from COMSOL modelling of the thruster magnetic topology. The magnetic field lines that close at the back of the thruster could cause the magnetization of the electrons near the cathode and it could be possible that electrons could not reach the beam ions by travelling across the magnetic field lines.

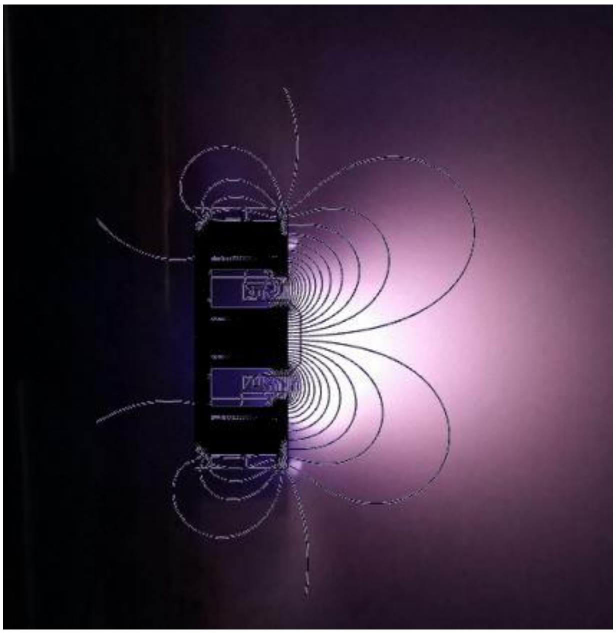

Figure 13. HK40 plume with magnetic contours

There are three types of electron motion in Hall effect thrusters: electron motion along the local magnetic field lines into the channel; closed drift, $\vec{E} \times \vec{B}$, motion around the channel; and cross-field (transverse) electron motion towards the anode [6]. The collisions with neutrals cause ionization in the channel. Electrons continue their movements generating cyclotron motion around the magnetic field lines and transverse motion towards the anode to close the electric circuit constructed between the anode and the cathode. However, if electron magnetization still exists near the anode, electrons fail to reach the anode and accumulate on magnetic lines, shadowing the anode voltage seen by cathode electrons. As could be seen in Fig.14, the discharge channel of HK40 would not be long enough for electrons to escape from magnetic field and reach the anode because magnetic field lines cross the anode.

For an ideal case, discharge current should be equal to the total electron current emitted. Ionization and perfect neutralization are achieved by the emitted electrons for this case. However, if emitted electron current is much lower than the electron current formed by ionization of the propellant, the electron current is not sufficient for the neutralization process as could be seen from Eq.5.

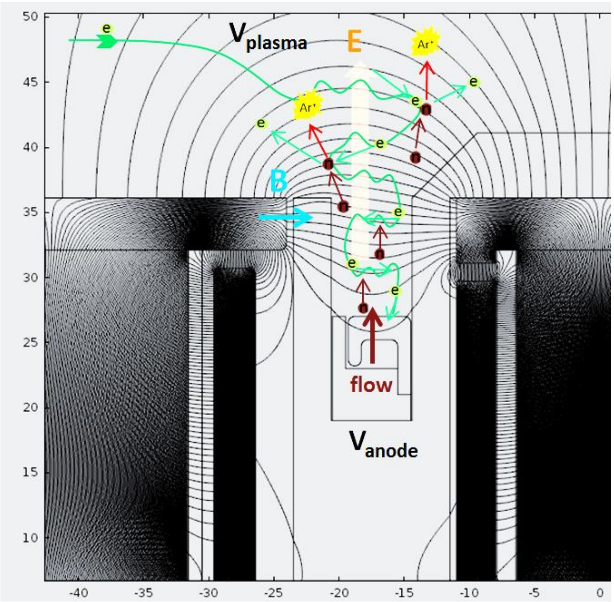

Figure 14. Depiction of the electron movement inside the channel of HK40

During the tests, it was observed that the electron current from the cathode is small compared to electrons coming from the ionization process. The beam current is calculated with Eq.4 by assuming poor neutralization, and the ratio of beam current to discharge current is sketched by considering different magnetic coil current values as in Fig.15. With the calculated beam current values, the ionization ratio of the propellant is calculated to be in the range of 75-80%. This explains high discharge current, since a flow rate of 18 sccm is supplied to the anode, electrons for the discharge come predominantly from the ionization process.

5. EFFICIENCY ANALYSIS

Beam current is calculated as the difference between the discharge current and cathode current as in Eq.4. For HK40 operation, it is assumed that the cathode could not provide sufficient electron for neutralization. All the cathode electrons are considered as contributing to the discharge current. Beam voltage is taken as the difference between the anode and plasma potentials without considering cathode coupling voltage. With these assumptions, thrust and total efficiency are calculated as in Eq's (8) and (9).

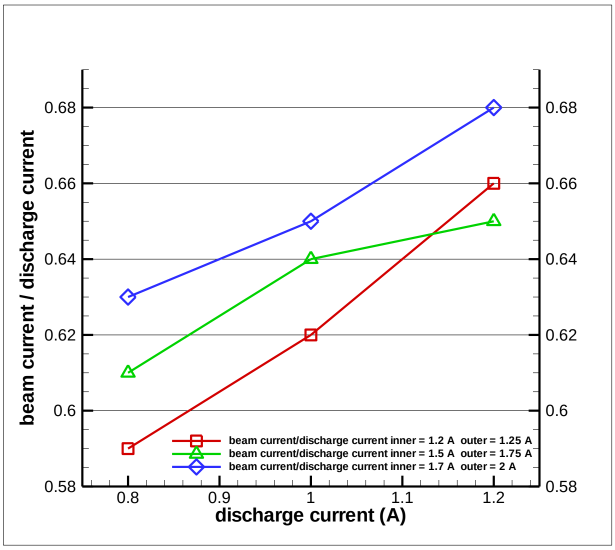

Figure 15. The current ratios for different magnetic field cases

The results are presented in Tab.1. The reference thruster while constructing HK40 was SPT-50 [7]. When compared to the operation parameters of SPT-50, HK40 is close to SPT-50 in terms of power consumption, thrust and the ratio of beam current to discharge current [7], [8]. However, it should be optimized regarding the mass flow rates, cathode current emission and magnetic structure.

6. CONCLUSION

In this study, experimental results for the testing of HK40 Hall thruster, a prototype Hall effect thruster developed at BUSTLab, operated with a prototype LaB_6 hollow cathode, also developed at BUSTLab, are presented. During the experiments various currents to and from the thruster and the cathode have been measured. The relations between the magnetic field and the discharge properties are studied by considering the emitted electron current. The measurement results along with relevant discussions are presented. After the tests, it was concluded that HK40 discharge channel should be redesigned and made longer, and the magnetic field along the channel be optimized accordingly. Also, the position of the cathode, which determines the parameter, R_c, can be varied to observe the changes in plasma potential and cathode voltage. As a result of the conducted experiments, certain optimizations are planned as future work.

ACKNOWLEDGEMENTS

This research is supported by Turkish Scientific and Technological Research Council (TUBITAK) under project number 112M862. The authors would like to thank Mert Satir for his contributions to this study. The authors also would like to thank Prof. Huseyin Kurt of Istanbul Medeniyet University for allowing the use of the computational facilities at Istanbul Medeniyet University and the COMSOL Multiphysics software for this study.

Table 1: Performance characteristics of HK40 Hall Thruster

$I_d(A)$	$V_a(V)$	$inner(A)$	$outer(A)$	$P_t(W)$	$I_b(A)$	$V_p(V)$	$T(mN)$	η_T
1.2	204	1.2	1.25	263.4	0.749	43.6	8.63	0.244
1.2	206	1.4	1.5	269.4	0.763	44.8	8.82	0.249
1.2	208	1.5	1.75	275.1	0.772	45.45	8.96	0.252
1.2	210	1	2	279	0.765	46.8	8.89	0.245
1.2	213	1.7	2	284.7	0.781	47	9.16	0.254

REFERENCES

1. Martinez-Sanchez, M. and Pollard, J.E., *Spacecraft Electric Propulsion-An Overview*, Journal of Propulsion and Power, Vol. 14, No. 5, 1998, pp. 688699.
2. Goebel, D. M. and Katz, I., *Fundamentals of Electric Propulsion: Hall Thrusters*, JPL Space Science and Technology Series, New York, USA, 2008.
3. Jameson, K, *"Investigation of Hollow Cathode Effects on Total Thruster Efficiency in a 6 kW Hall Thruster"*, Ph.D. Thesis, University of California, Los Angeles, CA, USA, 2008.
4. Courtney, D.G., *"Development and Characterization of a Diverging Cusped Field Thruster and a Lanthanum Hexaboride Hollow Cathode,"* M.S. Thesis, Massachusetts Institute of Technology, Cambridge, MA, USA, May 2008.
5. Jameson, K. K., Goebel, D. M., Hofer, R. R. and Watkins, R. M*., Cathode Coupling in Hall Thrusters.* 30th International Electric Propulsion Conference, Florence, Italy September 2007. IEPC-2007-278*.*
6. Kunning G Xu and Mitchell LR Walker. *Effect of External Cathode Azimuthal Position on Hall-effect Thruster Plume and Diagnostic*s. Journal of Propulsion and Power, Vol.30, No.2, 2014.
7. E. Ahedo and J.M. Gallardo. *Low Power Hall Thrusters: Physics, Technical Limitations and Design*. Micro-Propulsion Workshop, Lerici, Italy, May 2002.
8. Guerrini, G., Michaut, C., Dudeck, M., Vesselovzorov, A., and Bacal, M., *Characterization of Plasma Inside the SPT-50 Channel by Electrostatic Probes,* Proceedings of the 25th International Electric Propulsion Conference, 1997, pp. 1997-053